



Radiative and climatic effects of dust over West Africa, as simulated by a regional climate model

Fabien Solmon^{1,*}, Nellie Elguindi¹, Marc Mallet²

¹The Abdus salam International Center for Theoretical Physics, Strada Costiera 11, 34100 Trieste, Italy

²Laboratoire d'Aerologie, CNRS, Universite de Toulouse, 14 av. Edouard Belin, 31400 Toulouse, France

ABSTRACT: We used the Regional Circulation Model (RegCM) to investigate the direct effect of dust aerosol on climate over West Africa, with a specific focus on the Sahel region. First, we characterized the mechanisms linking dust radiative forcing and convective activity over Sahel and the net impact of dust on precipitation: The mean effect of dust over 11 summer seasons is to reduce precipitation over most of the Sahel region as a result of strong surface cooling and elevated diabatic warming inhibiting convection. However, on the very northern Sahel and in the vicinity of dust sources, a relative increase of precipitation is obtained as a result of enhanced diabatic warming in the lower atmosphere associated with high dust concentrations at low altitude. In the second part of the paper, we investigated the robustness of this signal with regards to different modeling conditions that are thought to be sensitive, namely the extension of the domain, the effect of dust on sea surface temperature, the land surface scheme, the convective scheme and the dust single scattering albedo. The simulated dust induced precipitation anomaly over West Africa is consistent and robust in these tests, but significant variations over the northern Sahel region are nevertheless pointed out. Among different factors, single scattering and surface albedo, as well as the nature of the convective scheme, have the greatest influence on the simulated response of West African climate to dust forcing.

KEY WORDS: Dust · Aerosol · Sahel · West Africa · Regional climate · Radiative effect · Single scattering albedo · Convection

— Resale or republication not permitted without written consent of the publisher —

1. INTRODUCTION

Dust aerosol direct radiative effects are thought to have a significant impact on West African regional climate and are likely to play a role in modulating seasonal precipitation over the Sahel region. Recent modeling studies suggest significant climatic effects of dust interacting with West African monsoon (WAM) dynamics from event to seasonal and climate scales (Miller et al. 2004a, Tompkins et al. 2005, Paeth & Feichter 2006, Yoshioka et al. 2007, Konare et al. 2008, Lau et al. 2009, Mallet et al. 2009, Perlwitz & Miller 2010, Stanelle et al. 2010, Lavaysse et al. 2011, Zhao et al. 2011). On the observational side, Klüser & Holzer-Popp (2010), analyzing different satellite observations, similarly concurred on a significant

impact of dust on cloudiness and precipitation over Sahel. All these studies outline the complex interaction between dust emission, transport, optical and hygroscopic properties, convective and land surface processes in shaping the regional climate response to dust. Consequently, the climatic signals obtained are subject to various sources of uncertainties, possibly leading to contrasting conclusions e.g. with regards to knowing if dust enhances or decreases annual precipitation in the Sahel region (Miller & Tegen 1998, Yoshioka et al. 2007, Lau et al. 2009).

As far as climate modeling is concerned, dust effects have been studied mostly with general circulation models (GCMs), which show that dust is able to induce circulation anomalies of large geographical extent over the Atlantic Ocean (e.g. Lau et al. 2009).

*Email: fsolmon@ictp.it

Fewer studies have used regional climate models (RCMs), which offer the advantages of an enhanced resolution for dust emission and transport processes, land surface gradients and weather system, but with the caveat of not capturing the full picture of dust induced anomalies. As an illustration, Sud et al. (2009) carried out a set of GCM numerical experiments in which they criticized any RCM approach to study aerosol climatic feedbacks because of forced boundary conditions.

In this context, we propose a study in which we are using the RegCM regional climate model to investigate the effect of dust on WAM and Sahelian precipitation. Extending the previous study of Solmon et al. (2008), we focus more specifically on the impact of different modeling conditions on the dust-induced climatic signal over the WAM domain. Among different factors, we selected those that seemed *a priori* the more sensitive, namely the geographical extension of the simulation domain, the possibility of dust feedback on sea surface temperature (SST), the land surface scheme and the convection scheme, as well as the dust optical properties. Through these sensitivity experiments, our final goal is to assess the robustness of the simulated induced climatic signal over Sahel and discuss sensitive factors.

In Section 2 and 3, we briefly introduce the RCM, the experimental setup used for this study, and we evaluate the quality of RegCM simulation over the domain. In Section 4, we discuss the simulated dust climatic signal over the WAM domain and the mechanisms involved. Section 5 is devoted to the investigation of the influence of the different modeling conditions on the dust climatic signal, while Section 6 discusses the significance of our results.

2. DESIGN OF THE EXPERIMENT

Our study is based on the regional modeling system RegCM extensively described by Pal et al. (2007) and Giorgi et al. (2012, this Special). The RegCM has been used for a number of years in a wide variety of applications (e.g. Giorgi & Mearns 1999, Giorgi et al. 2006). Of particular importance in this work, land surface processes can be simulated using the biosphere–atmosphere transfer scheme (BATS) scheme (Dickinson et al. 1993) or the CLM3.5 scheme (Steiner et al. 2009). The model also includes several cumulus convection parameterizations and notably the Grell (1993) and Emanuel (Emanuel & Zivkovic-Rothman 1999) schemes used in this study. All other model physics parameterizations are from the default version

of the model (Pal et al. 2007, Giorgi et al. 2012). Finally, the interactive dust aerosol emission and transport scheme used in this work is described by Zakey et al. (2006) and has been used in various studies (Konare et al. 2008, Solmon et al. 2008, Cavazos et al. 2009, Malavelle et al. 2011). The model uses 4 dust bins (diameters: 0.1–1, 1–2.5, 2.5–5, 5–20 μm) that are coupled to the radiative transfer scheme both in the shortwave (SW) and long wave (LW) part of the spectrum (Solmon et al. 2008). In the standard configuration, extinction cross sections for each bin respectively are 2.45, 0.85, 0.38, and 0.17 $\text{m}^2 \text{g}^{-1}$, single scattering albedos of 0.95, 0.89, 0.80 and 0.70, and asymmetry parameters equal to 0.71, 0.76, 0.81, and 0.87. However, single scattering albedos were modified in the specific experiment as described later (see Table 1).

The regional climatic impact of dust was assessed through a suit of numerical experiments for which 1 control simulation without dust and 1 simulation using interactive dust were performed. For each experiment, we then defined different simulation conditions in reference to a standard experiment (Table 1). The standard experiment corresponds to model physics options that have been used in the past to study both regional climate and dust effect over West Africa (i.e. Afiesimama et al. 2006, Solmon et al. 2008, Sylla et al. 2010). For each experiment, the dust climatic anomalies were defined as the difference between the dust (DUST) and control (CTL) simulations for a variable of interest (e.g. precipitation). As shown in Table 1 and developed in Section 5, we successively studied the impact of domain extension, SST cooling induced by dust, convection scheme, land surface scheme and dust absorption properties. All the experiments used NCEP reanalysis (NNRP2) as boundary condition forcing for years 1996 to 2006. Sea surface temperatures are normally prescribed as boundary conditions, and we used weekly NOAA OI-SST products (Reynolds et al. 2002). However, SST were perturbed in one of the experiments (cf. Table 1 and later discussion). We focus our discussion on the West African rainy season (June–August, JJA). The model horizontal resolution is 60 km.

3. SIMULATED AEROSOL OPTICAL DEPTH AND PRECIPITATION

3.1. Average dust aerosol optical depths

Fig. 1 compares the standard (STD) simulated dust aerosol optical depth (AOD) for the RegCM visible band with MISR satellite measurements at 500 nm

Table 1. Summary of the different numerical experiments. Simulations performed during 1996–2006, with forcing NNR P2, at a 60 km resolution. CTL: control, BATS: biosphere–atmosphere transfer scheme, SST: sea surface temperature, SSA: single scattering albedo

Experiment type and acronym	Simulation	Important physics options
Standard: STD	Control simulation: STD-CTL Dust activated: STD-DUST	BATS surface scheme Grell convection
Extended domain impact: EXT	Control simulation: EXT-CTL Dust activated: EXT-DUST	BATS surface scheme Grell convection
Aerosol SST feedback: SST	Control simulation: same as EXT-CTL Dust activated: SST-DUST	BATS surface scheme Grell convection Dust impact on SST (cf. Section 5.2)
Convection scheme impact: CONV	Control simulation: CONV-CTL Dust activated: CONV-DUST	BATS surface scheme Emanuel convection
Land-surface scheme impact: CLM	Control simulation: CLM-CTL Dust activated: CLM-DUST	CLM3.5 surface scheme Grell convection
Dust more absorbing: ABS	Control simulation: STD-CTL Dust activated: ABS-DUST	BATS surface scheme Grell convection DUST SSA -5%
Dust more diffusive: DIF	Control simulation: STD-CTL Dust activated: DIF-DUST	BATS surface scheme Grell convection DUST SSA $+5\%$

and a combination of MODIS Deep Blue over the continent and AQUA over ocean. These products have been chosen because they use retrieval algorithms that are able to quantify AOD over bright surfaces (Martonchik et al. 2004, Hsu et al. 2006), which is particularly important in the case of the Sahara desert. We focus here on a 4 yr average for JJA during 2003 to 2006. The average dust AOD results mainly from a succession of dust storm events of variable intensity and most often associated with African easterly waves (Jones et al. 2003). Although the online dust model is capable of simulating single episodes (Todd et al. 2008), it is beyond the scope of this study to discuss in detail any particular event, and we will focus more on the average quantities.

The MISR data show large AOD values, in excess of 0.4 (500 nm), over large portions of the Sahara (Fig. 1b). Two maxima can be identified: a primary maximum extending over the central regions of Mali and Mauritania, and a secondary one located between Niger and the Bodele depression in Chad. On MODIS Deep Blue, we noted that the Bodele region shows a larger AOD relative to the Mali/Mauritania region. AOD values are also slightly larger for MISR over the Sudan source region. Generally, the model shows consistency in reproducing the main emission areas, but tends to overestimate by ~ 10 to 15% the west Saharan source compared to observations. The model agreement is somewhat better when compared to MISR data, notably in the Mali/Mauritania region as well as the Sudanese part

of the domain. Over the Atlantic, the dust outflow is reasonably well simulated despite a 10 to 15 % overestimation directly linked to west Saharan source overestimation. Recent tests performed with RegCM4 and using experimental results of Sow et al. (2009) have shown that a possible source of overestimation might be linked to the simulated dust emission distribution, which could overestimate the fine dust fraction as also suggested by Kok (2011). This misrepresentation could also be responsible for smoother simulated AOD gradients linked to a larger proportion of small particles over the domain. Other sources of error could also be linked to simulated dry and wet deposition processes as well as variability of dust optical properties. These last remarks should be balanced by possible errors of satellite retrievals as illustrated by the variability between observations in Fig. 1. Finally, the possible contribution of biomass-burning aerosol transported from southern Africa (Tummon et al. 2010), which is visible on the satellite AOD, is not accounted for in the present experiment.

3.2. Average precipitation

First, we briefly discuss here the ability of RegCM to simulate the average West African climate and, in particular, precipitation over West Africa and the Sahel. Many studies have been focusing on this domain, outlining strengths and weaknesses of RegCM over this region (e.g. Sylla et al. 2010, Giorgi et al.

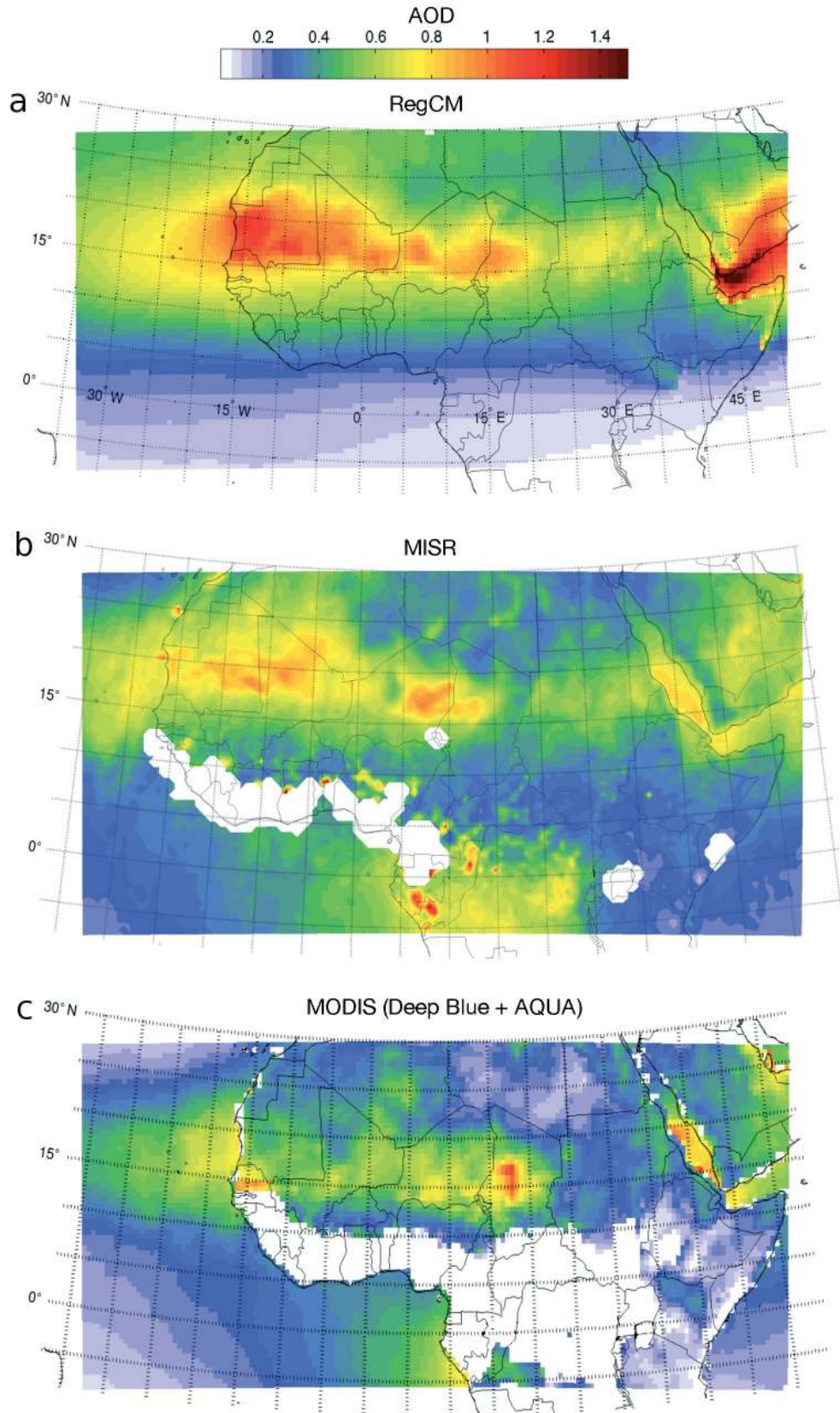


Fig. 1. (a) Simulated, (b) MISR, and (c) MODIS composite aerosol optical depth (AOD; unitless) for Jun–Aug (JJA) 2003–2006. Deep Blue product is used over land, and standard AQUA product is used over ocean

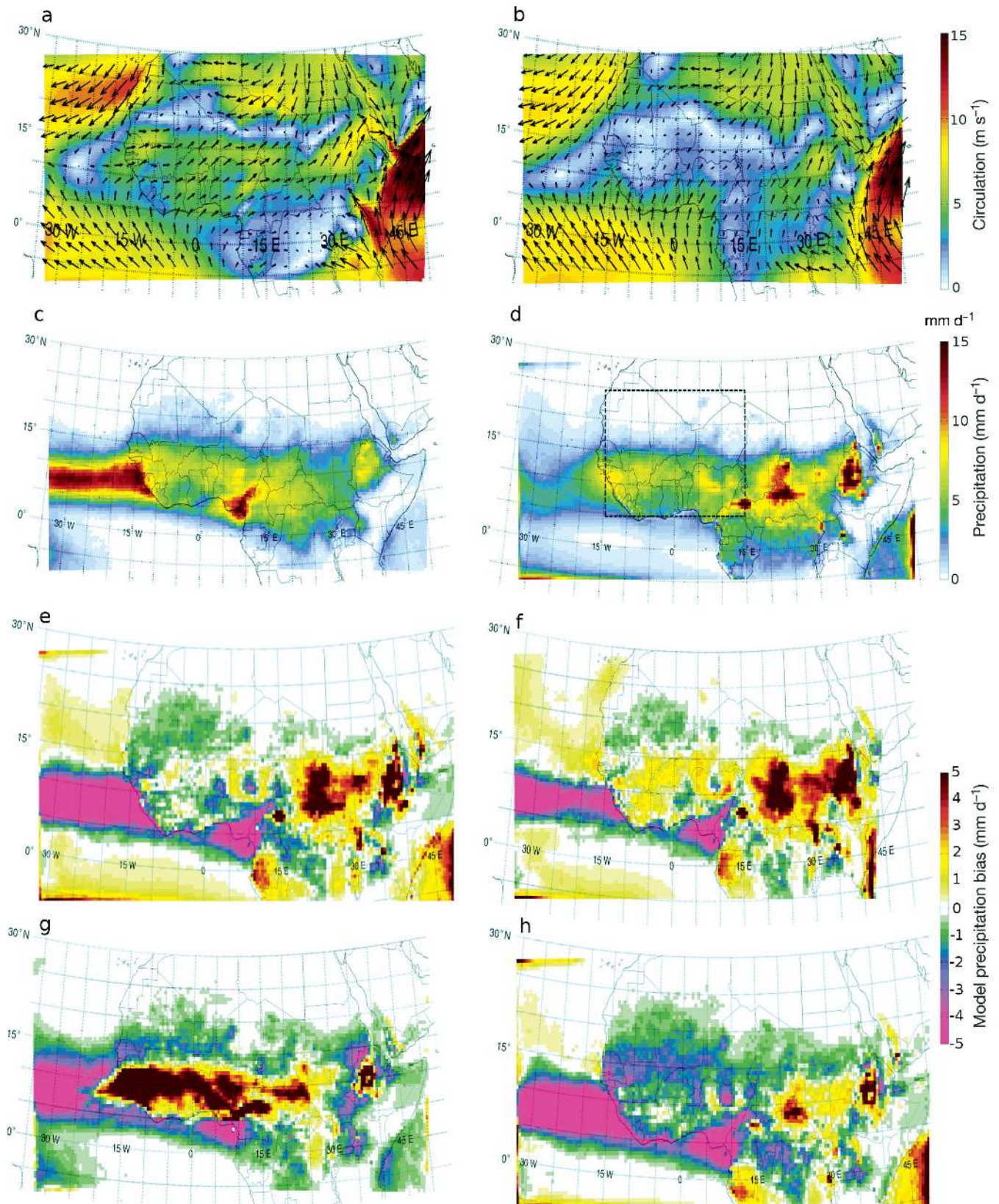


Fig. 2. (a) NCEP 2 reanalysis of mean circulation at 900 hPa for Jun–Aug (JJA) 1996–2006 (NNRP2 forcing). (b) Simulated mean circulation at 900 hPa for JJA 1996–2006 (standard control simulation: STD-CTL). (c) Observed precipitation (TRMM 3B42) for JJA 1998–2006 (d) STD-CTL simulated mean precipitation (RegCM) for JJA 1998–2006. Dashed box: West African monsoon region of interest. Model precipitation bias calculated from TRMM observation for JJA 1998–2006 with (e) STD-CTL simulation, (f) EXT-CTL simulation (note bias has been interpolated to a similar grid as STD experiment for comparison), (g) CONV-CTL simulation and (h) CLM-CTL simulation. See Table 1 for experiment acronyms

2012). Fig. 2b displays the STD-CTL mean circulation over the domain. For comparison we also plotted the NCEP2 reanalysis for the same period in Fig. 2a. Essential features of the West African monsoon mean circulation are consistently captured by the model, with southerly circulations dominating up to ~ 15 to 17°N , and northerly circulation characterizing the Harmattan flux to the north. Regional features like the Saharan heat low and the typical low level westerly jet $\sim 15^\circ\text{N}$ were also captured. Compared to NCEP2 reanalysis, however, we note that simulated monsoon flow is slightly overestimated over Sahel. More details on RegCM's ability to reproduce the WAM mean climate can be found in Sylla et al. (2010) and Konare et al. (2008).

Fig. 2c displays the simulated precipitation bias calculated from the tropical rainfall measuring mission (TRMM) 3B-42 observed precipitation product (Huffman et al. 2007) averaged for JJA during 1998 to 2006. Note that this period is actually shorter than the full simulation integration and model results were selected according to observed years. Large negative precipitation biases were obtained over the Gulf of Guinea and the Cameroon/Nigeria coastal regions of which precipitation are classically difficult to simulate. Over the ocean, the model clearly underestimates precipitation linked to the Intertropical Convergence Zone (ITCZ), which could be partly attributed to Grell convection scheme deficiencies when compared to other schemes, e.g. Emanuel convective scheme (cf. Section 5 in the present study, Giorgi et al. 2012). Over the WAM domain and in particular the Sahelian region, however, the model averaged precipitation is quite realistic with biases ranging from 5 to 15 % (see also Taylor diagram in Fig. 9). Over the northern Sahel (~ 15 to 18°N), the model actually underestimates precipitation compared to TRMM, which is already a very dry region. This feature is also observed in Giorgi et al. (2012) although they used different physics parameterization and boundary forcing. In the present study, our standard model configuration control simulation shows improved results over the Sahel and the WAM domain compared to previous studies using RegCM3 (Afiesimama et al. 2006, Konare et al. 2008), which were systematically overestimating the strength of the monsoon and precipitation intensities. The use of a more realistic desert albedo used as part of the BATS surface scheme over this region is one of the main factors for this improvement in the recent version of the model. Steiner et al. (2009) also showed drastic improvement using CLM3.5 versus BATS land surface scheme partly attributable to the use of refined

surface parameters. In line with this last remark, we report in Fig. 2f the precipitation bias using the CLM-CTL run in comparison to STD-CTL. Differences between the 2 schemes are minor in our case; regionally we note a reduction of precipitation overestimation over Sudan as well as a slight drying over Sahelian regions when CLM3.5 is used. The influence of domain extension (experiment EXT) in terms of spatial correlation coefficient and RMSE is also minor with values quite close to the STD experiment (Figs. 2d & 9). However, the bias pattern for the EXT-CTL is slightly positive when it tends to be negative in the STD experiment (Fig. 2c,f), which by definition is not reflected by the RMSE. As expected, the choice of the convection scheme appears to be a much more sensitive issue (Figs. 2e & 9). Precipitation in the Sahel region is strongly overestimated when the Emanuel convection scheme is activated, leading to a large RMSE; however, the spatial correlation coefficient is quite good. Note that for sub-regions of the domain, like the ocean and equatorial forest, the Emanuel scheme performs better than Grell when compared to TRMM data. This behavior of the RegCM/Emanuel convection configuration over the region has been pointed out in different studies (Pal et al. 2007, Sylla et al. 2010). However, despite this large bias, we decided to keep this simulation since we wanted to assess in fine detail the relative impact of dust radiative effects when the convection scheme differs: The CONV experiment provides hence a context where convection triggering and amplitude is more intense compared to the STD experiments.

4. DUST INDUCED CIRCULATION AND PRECIPITATION ANOMALIES

In this section, we investigate the effect of dust aerosol on mean regional dynamics and precipitation over the West African domain by comparing the CTL and DUST standard case simulations. As shown in Fig. 3b, the main effect of dust radiative forcing is a reduction of simulated precipitation over the Sahel region, especially between 5 and 15°N . The decrease of precipitation is associated with a circulation anomaly opposed to the normal monsoon circulation, meaning a monsoon weakening in this case, and a mean sea level pressure increase over land (Fig. 3a). Over the ocean, the picture is quite different and results will be discussed in more detail in Section 5. Over the Sahelian region and the WAM domain, similar circulation anomaly patterns have been obtained

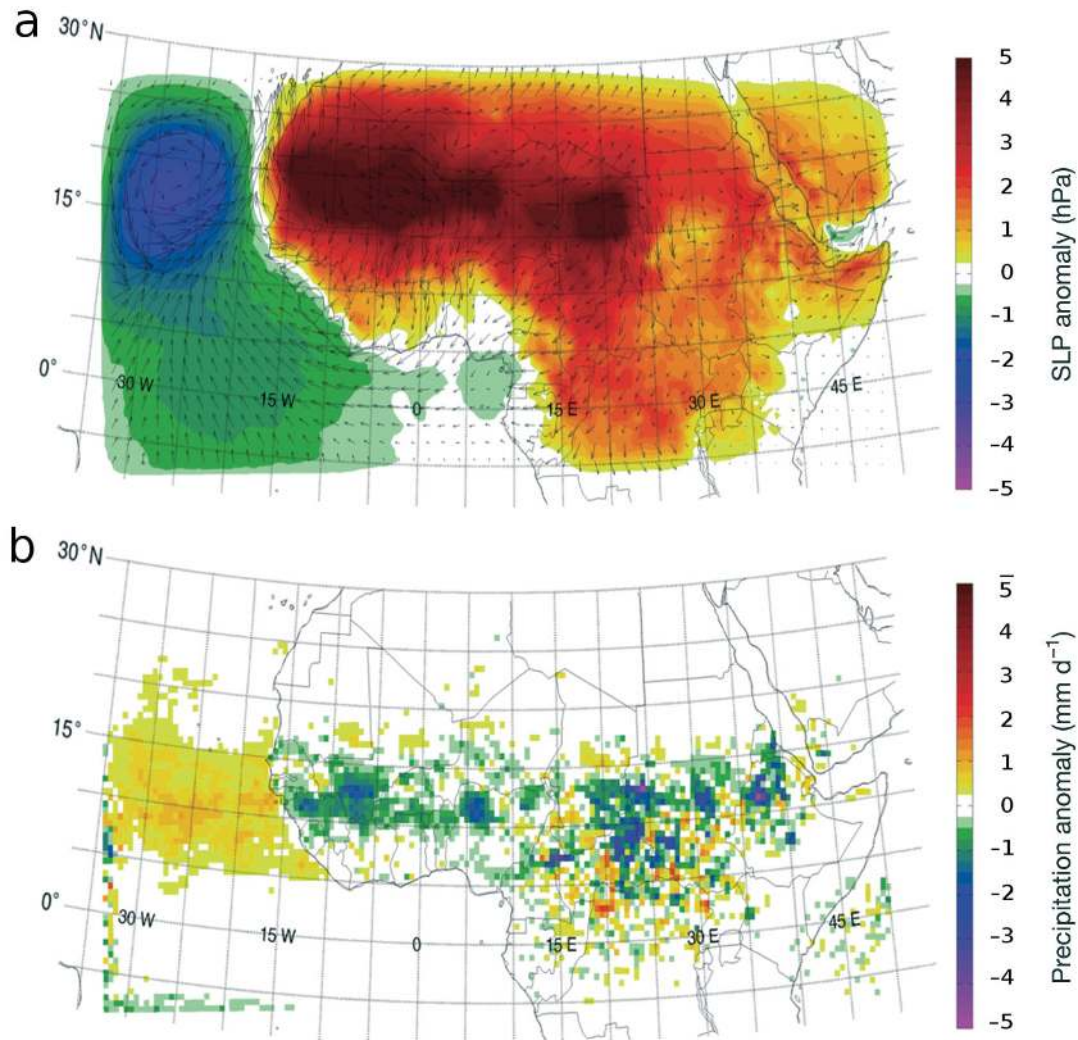


Fig. 3. (a) Sea level pressure (SLP) and circulation at 850 hPa anomaly for the standard experiment. Anomaly = STD-DUST – STD-CTL. (b) Precipitation anomaly for the standard (STD) experiment. Both panels: Jun–Aug (JJA) 1996–2006

by Zhao et al. (2011) using WRF-chem regional integration. To further understand the simulated average dust effects in the continental WAM region, we examined meridional cross sections of dust induced anomalies of diabatic heating rates associated with vertical turbulence (Fig. 4a), radiation (Fig. 4b) and convection processes (Fig. 4c) as well as the corresponding meridional precipitation anomalies (Fig. 4d). These diagnostic quantities have been obtained by taking the difference of STD-DUST and STD-CTL simulated heating rates zonally averaged between and 15°W and 15°E for JJA of 1996 to 2006. The large dust extinction of downward SW radiation induces a surface cooling anomaly and a reduction of surface sensible and latent heat fluxes. This cooling anomaly affects the lower troposphere, heat turbulent transfer being reduced in the DUST case (Fig. 4a). The meridional distribution of the cooling anomaly is

shaped first by dust AOD, with stronger downward SW extinction for larger AOD (over Sahara) but also by the surface albedo, with a negative surface radiative forcing being larger over darker Sahelian vegetated surfaces compared to the brighter desert (Liao & Seinfeld 1998, Miller et al. 2004). On average, the turbulent cooling anomaly tends to be maximally ~15°N in our simulations and its vertical extension depends on the intensity of the turbulent transfer. Note that in the thermal (i.e. LW) part of the spectrum, dust induces a relative warming at the surface (positive surface LW radiative forcing), especially during the night time. However, in our simulations, surface cooling SW effects are on average dominant and offset LW effects (data not shown).

Since dust particles are not purely scattering, they also induce a SW radiative diabatic warming in the atmosphere via radiation absorption processes (Liao &

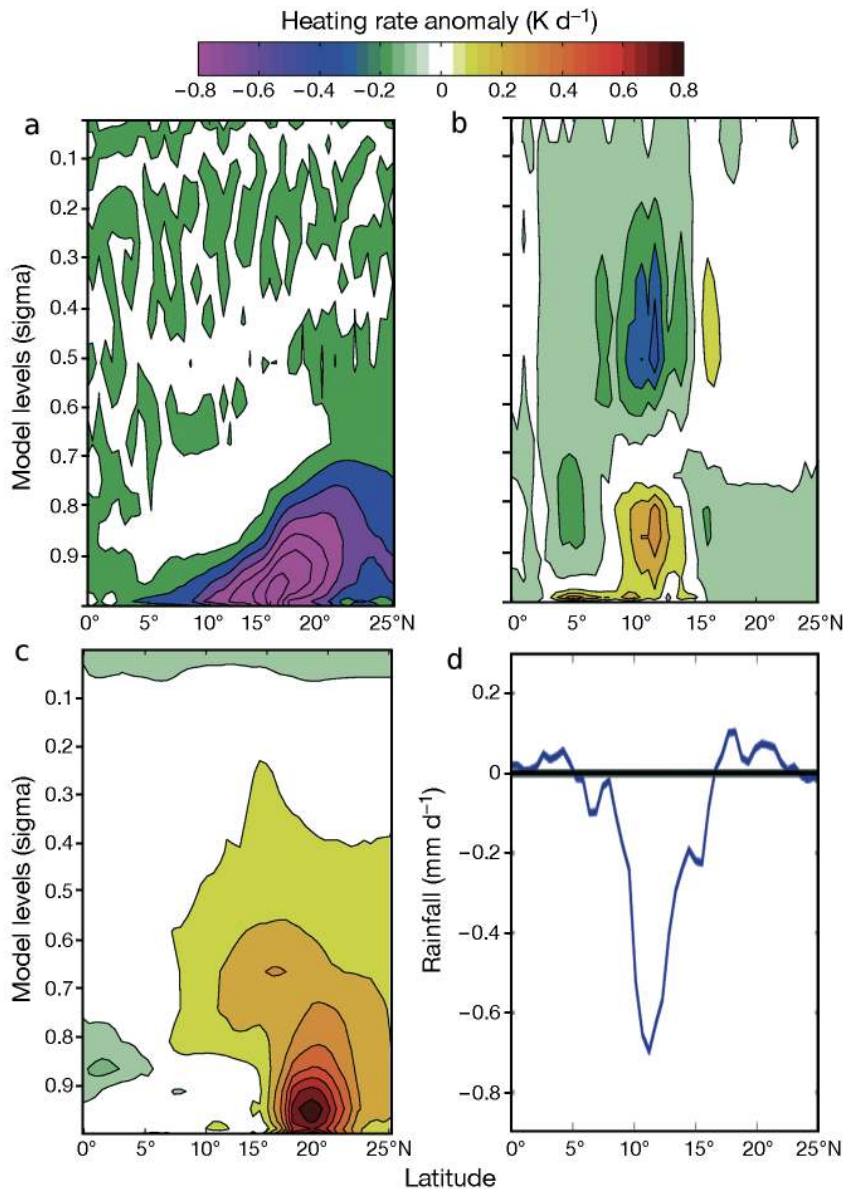


Fig. 4. Meridional cross section of heating rates and precipitation anomalies calculated from the standard (STD, DUST-CTL) experiment for Jun–Aug (JJA) 1996–2006 and spatially averaged for 15°W–15°E (see box in Fig. 2d). (a) Turbulent mixing, (b) convective, and (c) radiative heating rate anomalies. (d) Corresponding precipitation anomaly (DUST–NODUST)

Seinfeld 1998). Fig. 4b represents the meridional cross section of the simulated vertical radiative heating rate anomaly, which primarily depends on the dust concentration distribution and absorption optical properties. Consequently, the maximum heating anomaly is obtained in the lower atmospheric layer in the vicinity of the mean Saharan sources ($\sim 0.8 \text{ K d}^{-1}$ between 15 and 20°N). This warming anomaly extends to the middle troposphere and also southward to $\sim 5^\circ\text{S}$ above the mean monsoon layer. This type of stratification has been pointed out in recent modeling and ex-

perimental studies (Osborne et al. 2008, Stanelle et al. 2010). Note also that smaller contributions induced by climatic feedbacks notably on water vapor and cloud fields can contribute secondarily to the SW radiative heating anomaly, which could explain the negative values seen in Fig. 4.

Turning our attention to convection that basically reacts in function of the forcings discussed above, we can see 2 kinds of patterns emerging from convective heating rate anomalies (Fig. 4c). Up to $\sim 15^\circ\text{N}$, we obtain a vertical dipole structure showing a cooling anomaly in the middle/upper troposphere. This indicates a more shallow convection, less heat being released by convective processes in the upper atmospheric levels. Convective inhibition is linked here to the combined effect of lower tropospheric cooling (Fig. 4a) and elevated radiative warming in the dust layer (Fig. 4b), leading to more stable conditions on average. The inhibition of Sahelian convection is also related to the decrease of the monsoon pump intensity and circulation and pressure anomaly shown in Fig. 3.

However, north of 15°N, we observe that this pattern reverses and, although the signal is weaker, a slight enhancement of convective activity is obtained (Fig. 4c). This enhancement is due to improved warming occurring lower in the atmosphere as one gets closer to the dust source and secondarily to a relative decrease of dust surface cooling efficiency as one moves towards higher soil albedos. These conditions lead to a more favorable environment for convection triggering (Miller et al. 2004).

However, this effect is rather limited since environmental conditions are becoming dryer and on average less convective $>15^\circ\text{N}$ compared to further south. Similar responses have also been outlined at the scale of specific dust events (Stanelle et al. 2010) and are analogous to effects described in Miller et al. (2004) and Lau et al. (2009).

In Fig. 4d, the zonal precipitation anomaly matches the convective heating rates anomaly perfectly, with dust inducing drying over the Sahel and West Africa and a slight precipitation enhancement above 15°N.

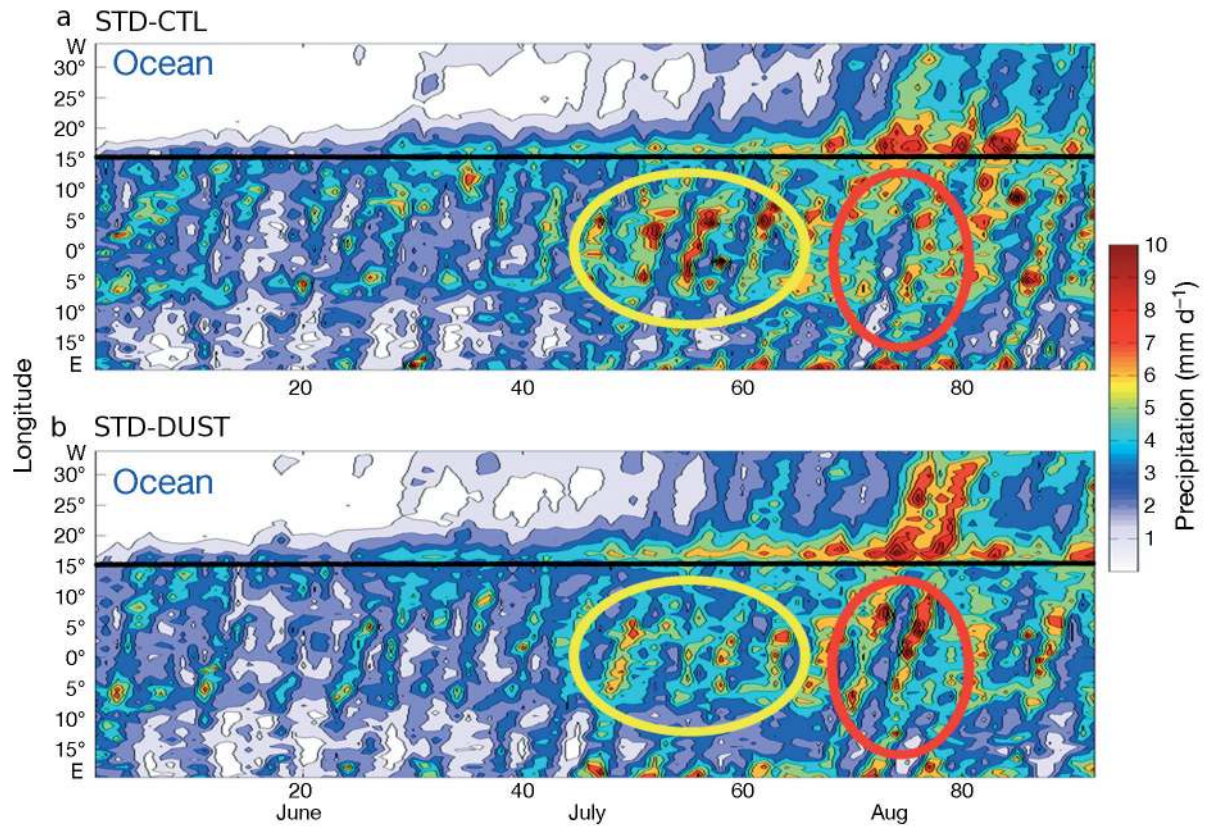


Fig. 5. Time–longitude diagram of precipitation for Jun–Aug (JJA) 2006, averaged for 10–22°N region for the (a) standard control (STD-CTL) and (b) standard dust (STD-DUST) simulation. Yellow circles: decreased precipitation by dust. Red circles: increased precipitations. Day 1 = 1 June. Area above 15° W = ocean

Turning our attention to the seasonal variability of simulated precipitation, Fig. 5 displays individual patterns related to the dust effect on African easterly systems showing both precipitation decreases and sometimes increases in the STD-DUST simulation compared to STD-CTL. In this specific example, cases of increased precipitation seem to occur later in the season as in August when the northward penetration of the monsoon front, and associated low pressure system track, is maximum and closer to dust sources, where dust diabatic heating is larger. This situation could then offer a context where convective triggering by dust can be more effective. However, this latter argument would need a deeper analysis.

5. ROBUSTNESS OF THE SIMULATED DUST INDUCED SIGNAL

5.1. Effect of simulation domain

Studying the effect of any perturbation with a regional climate model poses *a priori* a theoretical problem because dynamical feedbacks and anom-

alies induced by a perturbation (whether it is dust or landuse change experiments, for example) cannot freely develop beyond boundaries. As discussed by Sud et al. (2009) and Lau et al. (2009), Saharan dust can induce large dynamic anomalies over the tropical Atlantic, which can then feedback on the West African monsoon through, for example, a modification of on-shore moisture fluxes. To test the potential impact of domain boundaries on the dust climatic response over Sahel, we performed a simulation on an extended region (EXT experiment) depicted in Fig. 6a,b. This experiment does not account for possible teleconnection through eastern, northern and southern boundaries as a GCM would allow (Rodwell & Jung 2008) but constitutes a first order sensitivity test.

Turning our attention to dynamical responses, the most striking feature when comparing Fig. 6a and Fig. 4a is the extension of a large cyclonic anomaly over the Atlantic Ocean that is barely visible in the standard experiment due the model boundary. The cyclonic anomaly is associated with a rising motion induced by dust diabatic heating and positive convection feedback (data not shown), as well as a

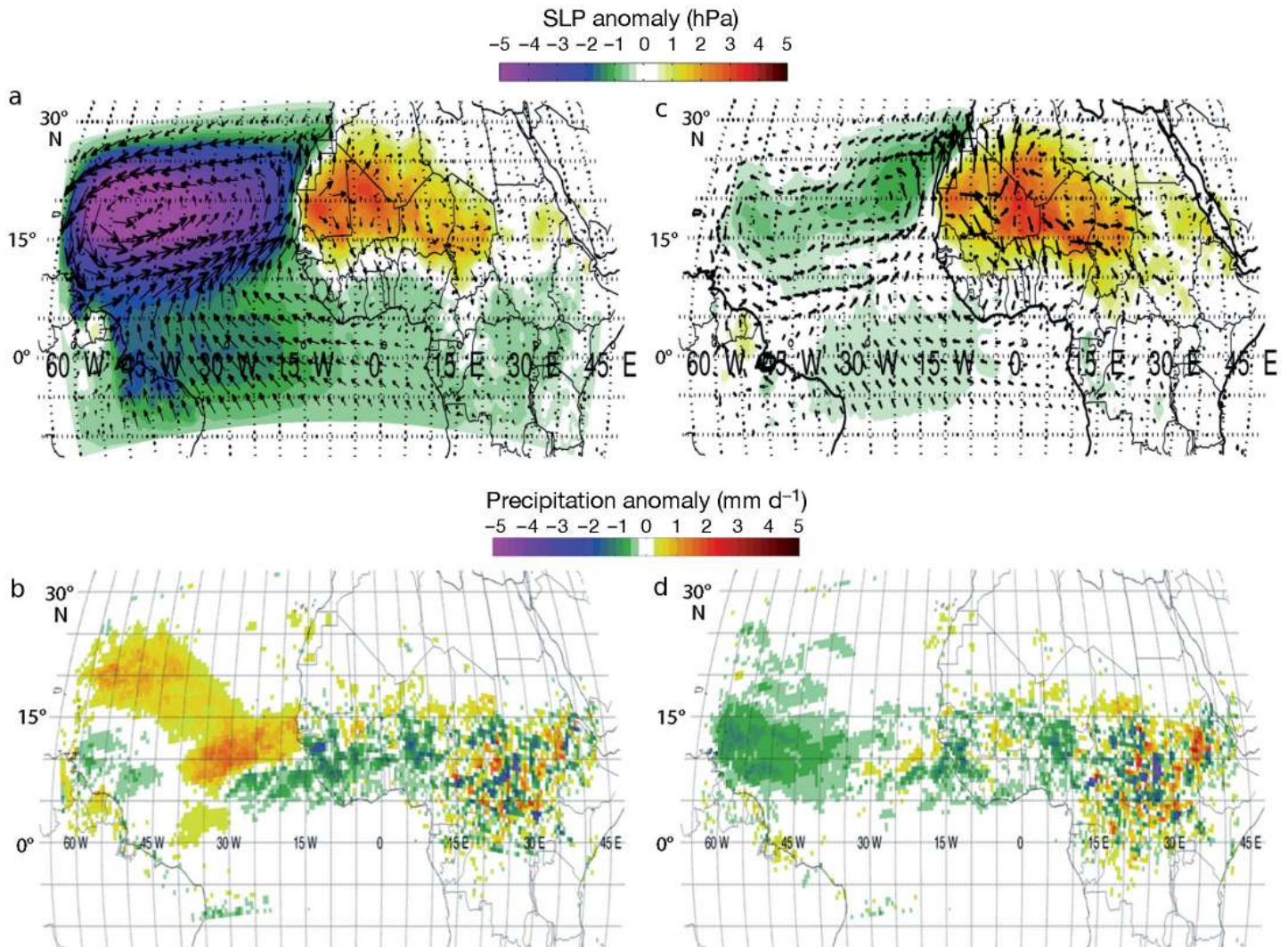


Fig. 6. DUST-sea level pressure (SLP) and 850 hPa circulation (vectors) anomalies in the (a) extended domain experiment, (EXT) and (c) SST experiment, and their respective (b, d) precipitation anomalies. All data for Jun–Aug (JJA) 1996–2006

northward shift of the ITCZ precipitation band and an increase of precipitation over the ocean. Over the ocean, this pattern is consistent with the discussion of Wilcox et al. (2010) and similar anomalies have also been obtained by Lau et al. (2009). However, contrary to Lau et al. (2009), we find a sharp reversal of this pattern as we go from ocean to continent, where the pressure anomaly becomes positive and is associated with diverging and anticyclonic patterns indicating a decrease in monsoon intensity as discussed for the STD experiment. Consistently, the EXT precipitation anomaly obtained over the Sahel shows a pattern relatively similar to the STD experiment with a dominant drying effect over West Africa and the Sahel (Fig. 6b). We note that both the positive and negative rainfall anomalies reach the same magnitude, and the drying pat-

tern tends to extend a bit more southward in the case of the EXT experiment (see Fig. 8a,b). Overall, despite the fact that dust induces a significant model response extending far over the tropical Atlantic, this response does not seem to have drastic feedback on the rainfall anomaly over the Sahelian region. The interpretation of these results is that the dominant effect of dust direct and semi-direct radiative perturbation is primarily occurring through the modification of regional convection over the Sahel and ensuing impact on WAM dynamics as discussed in Section 4. Long range feedbacks resulting from remote environment modifications, e.g. moisture flux modification associated with the cyclonic anomaly over the ocean, may contribute to the signal but appears to be secondary for Sahelian regions.

5.2. Impact of dust-induced SST cooling

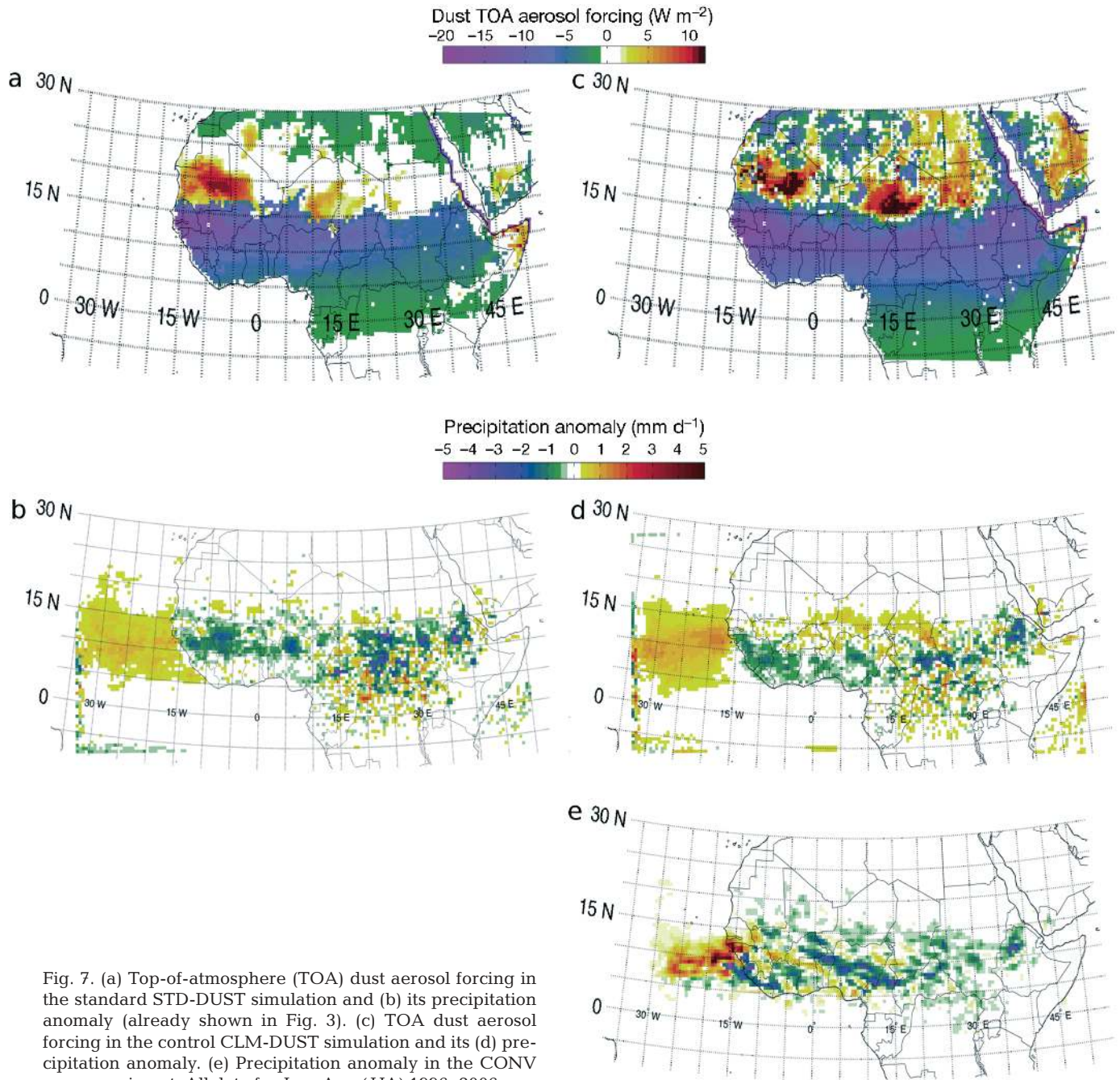
In line with the above discussion, one of the potential limitations of the regional model is the fact that SSTs are prescribed in the STD experiment and do not feedback to dust radiative extinction. This basically creates an energetic imbalance at the ocean. Diabatic warming effects are not compensated by an expected decrease of SSTs and cooling of the marine boundary layer due to dust, and ensuing circulation and positive precipitation feedback discussed in Section 4 might be thus overestimated (Miller et al. 2004b). Calculating the impact of dust on SSTs can be achieved using a regional climate–ocean coupled model that was not available at the time of this study despite recent developments (Ratnam et al. 2009, Artale et al. 2010). Alternatively we conducted here a simple first order experiment in which we decreased the SST as a function of AOD (0.8K per unit dust AOD) to mimic the effect of downward SW reduction due to dust. This value was chosen as a reasonable value when compared with other studies using a slab ocean model and observations (Martínez Avellaneda et al. 2010). When averaged, the obtained mean JJA SST anomaly ranges between 0 and 0.65K and shows the same gradient as dust AOD. We emphasize the fact that no energy balance is performed to constrain the evaporation flux beneath the dust layer with this method. Other caveats of this method are in the fact that SSTs are instantaneously reduced when high AOD events occur, whereas in reality, ocean dynamics and thermal inertia induce regional modulations and slower responses of SSTs to surface radiative forcing. For the SST experiment, we also used the extended simulation domain, which maximizes the oceanic area impacted by dust. The SST experiment should thus more appropriately be compared with the EXT experiment rather than STD in this case.

Fig. 6c,d display the circulation and precipitation anomaly obtained in the SST case and we can observe that over the ocean, a reduction of precipitation is now obtained, which is essentially opposite to the EXT experiment response. Despite the simplicity of the approach, this result is in-line with Yue et al. (2011) who obtained a similar response using a GCM coupled to a slab ocean model. In terms of circulation anomalies, it is worth noting that we still obtain a slight cyclonic anomaly that could be *a priori* counter intuitive. Dust diabatic warming still results in a slight enhancement of mean ascending motion in the lower troposphere, but on the other hand, the reduction in latent heat flux induced by the drop in SSTs could significantly reduce available moisture for deep

convection events controlling precipitation. However, over the Sahelian region we observe that the inclusion of interactive SSTs did not significantly change the nature of the precipitation anomaly compared the EXT control simulation (Fig. 6b,d). In this experiment, the modification of evaporation over the ocean matters less than regional and continental mechanism for determining the precipitation response over Sahel. The mean drying effect obtained in the SST experiment is perhaps less pronounced than in the EXT experiment, which could be due to the fact that the dust surface cooling differential between land and ocean is less contrasted in the SST case compared to the EXT case. In addition, the SST case simulation is by definition drier since the input of moisture via surface evaporation is reduced due to the decreased SSTs.

5.3. Effect of land surface scheme

The surface scheme is thought to be of great importance for simulations of West African climate (Zheng & Eltahir 1998). Surface parameterizations can directly affect dust emissions through soil properties (soil texture, humidity, roughness) and indirectly via climatic feedback on surface wind. Dust radiative forcing also greatly depends on the soil albedo (Tegen & Lacis 1996, Liao & Seinfeld 1998). In the CLM experiment, we test the impact of using the CLM3.5 land surface parameterization instead of BATS in the STD experiment (Table 1). However, there are only limited differences in terms of dust emission, since the dust emission scheme is based on high resolution texture maps independent from the choice of BATS or CLM3.5. The only differences in emissions arise essentially via climatic feedback on surface wind speed and soil humidity. As discussed in Section 3.2, the mean climatology is also relatively similar between the 2 model configurations. However, turning our attention to top-of-atmosphere (TOA) radiative forcing fields, the CLM experiment shows more extended and larger positive TOA forcing over the desert, meaning in this case more of a warming effect in the vicinity of dust sources (Fig. 7a,c). These differences are primarily due to differences in surface albedo fields that are higher in the sandy desert emission region in the CLM3.5 case, and to a lesser extent slightly higher simulated dust load in source regions (e.g. Bodele region, data not shown). If we now analyze the precipitation anomalies (Fig. 7b,d), we can see that a similar pattern is obtained in the CLM experiment but with a south-



ward shift (by ~ 3 to 4°) compared to the STD experiment. This shift is also clearly visible on the meridional cross sections (Fig. 8a,d), and we also note that the drying effect/precipitation enhancement effect are also slightly weaker/larger in the CLM case. This pattern is consistent with the relative enhancement of positive TOA forcing in the Sahara/northern Sahel region, which means in this case a relative increase of diabatic warming versus surface cooling with ensuing effects on convection as discussed in Section 4.

5.4. Effect of convective scheme

As seen in Section 3.2, convection is an essential process in the precipitation response to dust radiative forcing. For the present section, we performed an experiment in which we used the Emanuel scheme instead of the standard Grell scheme. As discussed in Section 3.2, the Emanuel scheme is generally more intense over the region in terms of convective triggering and precipitation intensity. Fig. 7e represents

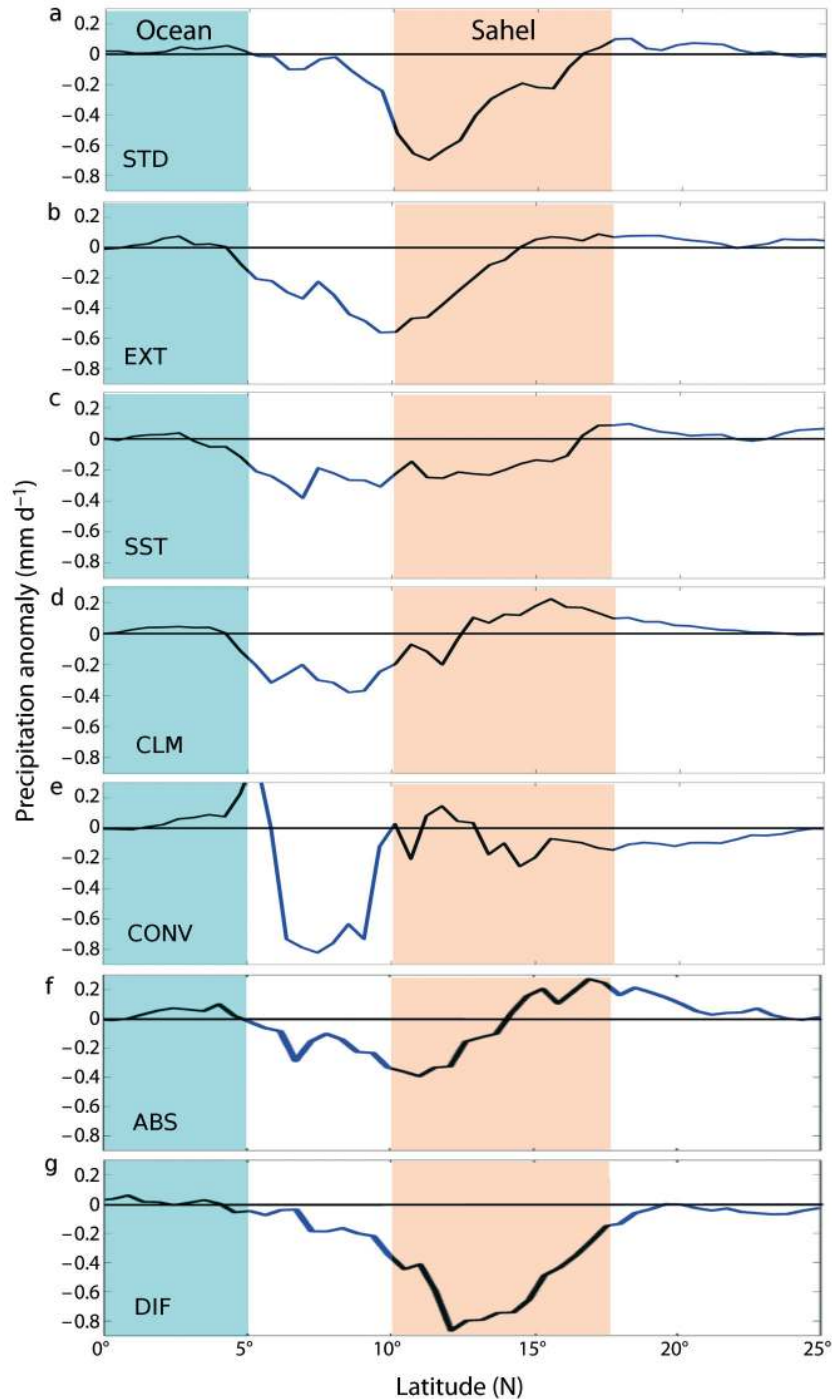


Fig. 8. Meridional cross sections (15°W – 15°E average) of mean precipitation dust induced anomalies for Jun–Aug (JJA) 1996–2006 and for each experiment (a–g) as defined in Table 1

the precipitation anomaly obtained in the CONV experiment. Over the Sahelian domain, the response is much noisier than in the standard case (Fig. 7b) perhaps due to a larger sensitivity of the convective regime when using the Emanuel scheme, which enhances stochasticity in the response. However, over most of the continental domain and especially

Sahelian regions in Fig. 7e, a reduction of precipitation is the dominant signal. On the meridional cross section (Fig. 8e), this signal is perhaps less evident due to the fact that the 15°W – 15°E longitudinal average includes coastal locations ~ 10 – 15°N , which actually shows a large convection and precipitation enhancement induced both by the sensitivity of the

Table 2. Average impact of dust aerosol in the different experiments for the Sahel and northern Sahel region. Precipitation differences have been averaged between 15° W and 15° E. See Table 1 for experiment acronyms

Experiment	Precipitation anomaly (%) (~10–17° N)	Precipitation anomaly (%) (~15–17.5° N)
STD	–6.8	–7.5
EXT	–3.2	+3
SST	–3.3	–1.6
CONV	+3.7	+25.6
CLM	–1.3	–9
ABS	–0.9	+27.4
DIF	–11.4	–49.1

Emanuel scheme and the fact that only diabatic warming plays a role as discussed in Section 5.2. The absolute change of precipitation might seem of bigger amplitude in the CONV experiment, but since the rainfall is larger, the relative change is not significantly different compared to STD experiment (Table 2), at least for continental regions. Overall, the choice of convection scheme is certainly an important factor that can modulate simulated dust induced precipitation anomalies. Nevertheless, in our case, the continental drying still appears to be a robust pattern. Over the ocean, the significant precipitation enhancement is also a consistent pattern compared to the standard experiment but cannot be qualified as robust as shown by the SST experiment.

5.5. Effect of dust absorption optical properties

We complete the sensitivity studies by examining the possible effect of dust absorption properties on the precipitation anomaly. Since this topic has been specifically developed in Solmon et al. (2008), we just briefly discuss the results obtained here. Fig. 8 represents the meridional cross section obtained when varying the dust single scattering albedo (SSA) by $\pm 5\%$, which is equivalent to consider more absorbing versus more diffusive dust aerosols. This range of variation is representative of the variability of published SSA values, which exhibit natural variability linked to dust mineral composition, size distribution or possible coating processes during transport. Compared to the standard simulation, more absorbing dust induces a relative enhancement of diabatic warming, which results in a relative enhancement of the northern precipitation increase signal and a relative decrease of the dust drying effects, with overall a

southward shift of the STD pattern. The response is very similar to the CLM experiment since ‘darkening’ the aerosol or ‘brightening’ the surface have similar effects from the radiative forcing point of view (see also Miller et al. 2004). At the other end of the spectrum, increasing the SSA up to obtaining an almost purely scattering dust inhibits the positive convection response and increases the drying effect, since in this case the aerosol diabatic warming becomes very small in comparison to the SW extinction at the surface (Solmon et al. 2008, Lau et al. 2009). Overall, given the range of variation we considered here, the SSA appears to be a very sensitive parameter when compared to the other experiments of this study.

6. SUMMARY AND CONCLUSION

Fig. 8 summarizes the dust precipitation anomalies obtained for the different experiments, and Table 2 shows the corresponding relative change in precipitation for the Sahelian and northern Sahel bands. Over the WAM domain, the anomalies obtained show a similar dipole pattern that thus appears to be robust with regards to different modeling conditions. Only in the convection experiment is this pattern perhaps less obvious, but we point out the noisier response indicating that a longer integration is probably necessary, as well as the lesser quality of the control simulation in this case. Overall the general simulated patterns are consistent with other studies that conclude a northward shift in the precipitation belt induced by aerosols (Miller et al. 2004, Perlwitz & Miller 2010). Quantitatively, the drying effect appears to be more important over the WAM domain, but in terms of relative precipitation, precipitation changes are still significant (Table 2). However, looking in particular at the Sahelian region (Fig. 8), we see that the conditions of the simulations are important and that the limit between positive and negative precipitation feedback can vary significantly according to land surface conditions and dust optical properties. The very northern Sahel is also the region where the relative impact of dust is maximum (Table 2), which from an impact perspective is important here since precipitation is scarce. Dynamic downscaling climate models focusing on this sensitive region should definitely account for dust aerosol as an important factor, together with land use conditions. In Fig. 9’s Taylor diagram we can appreciate the impact of dust compared to control simulations and observations as well as the modulations brought

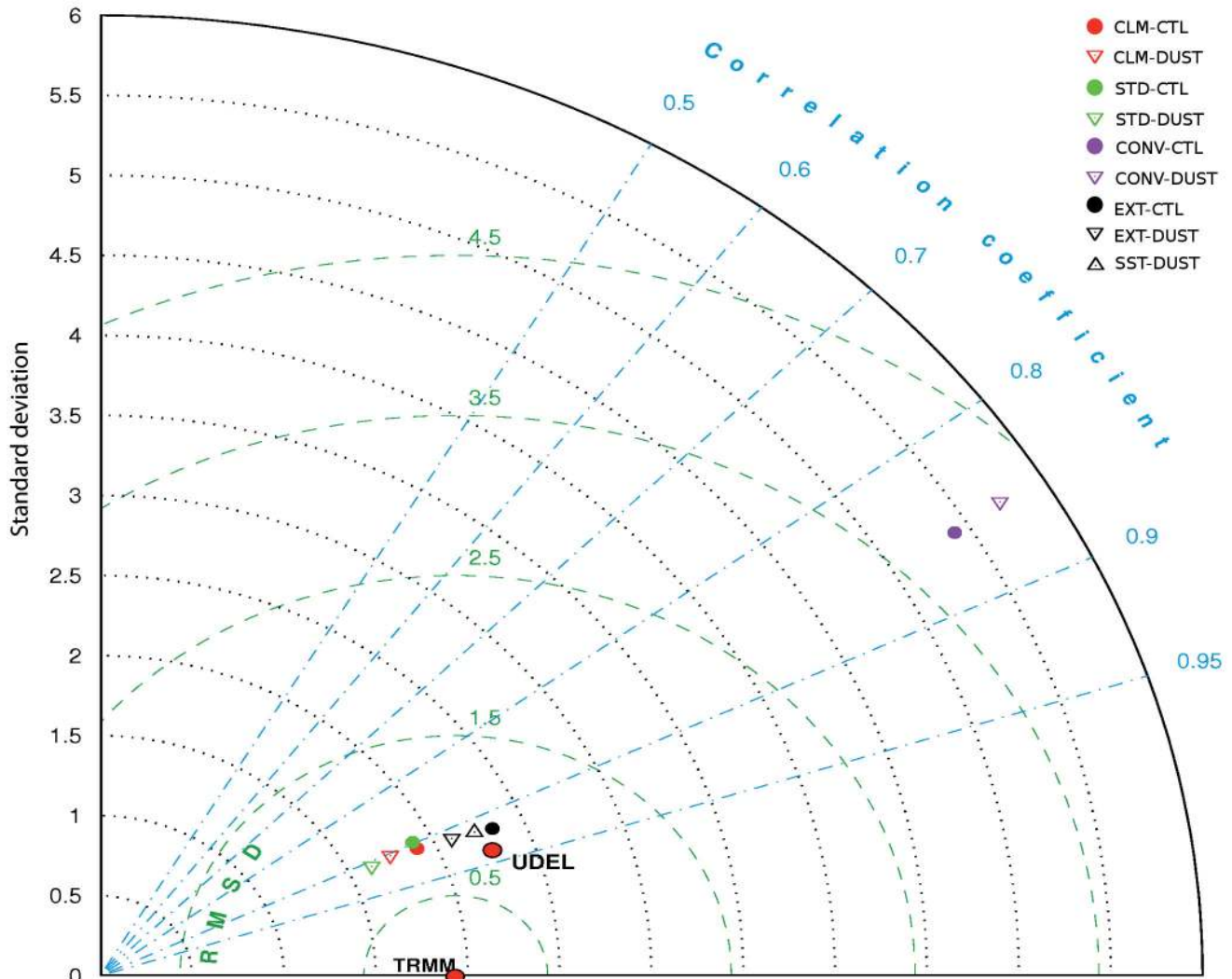


Fig. 9. Taylor diagram showing simulated Jun–Aug (JJA) 1998–2006 precipitation spatial correlation coefficient, root mean square deviation and SD calculated with regards to TRMM observations. The University of Delaware (UDEL) precipitation data set is plotted for comparison with TRMM. Statistics are calculated over the Sahel box (15°W – 15°E , 10 – 17°N) and represent simulations performed in the different experiments, including dust (-DUST) or not (-CTL) (cf. Table 1)

by different modeling conditions. To characterize the observation variability, we also plotted statistics relative to the University of Delaware (UDEL) precipitation data set (Legates & Willmott 1990). We cannot conclude whether or not there is a clear improvement in the dust versus control simulations compared to TRMM observations here. It should be noted in this regard that discrepancies between different simulation results and TRMM observations (as measured by the distance between simulations and TRMM on the diagram) almost compare with differences between TRMM and the UDEL alternative precipitation data. This implies that measurement of the impact of dust on the quality of the RegCM precipitation simulation depends on the observational data set chosen as a reference. Nevertheless, we can see in Fig. 9 that

the relative impact of dust, measured by the distance between DUST and respective CTL simulations, is of the same magnitude as the impact of using a different land surface scheme as measured by the distance between the STD-CTL and STD-CLM simulations. This, however, does not hold for convection, dust impact being of less importance when compared to the variability introduced by the choice of the convection scheme.

However, the relatively limited impact of dust on average precipitation ($<10\%$ over the Sahelian box) should be balanced by several remarks. First, the results might also be resolution-dependant with possible higher impacts as the meso-scale system becomes better resolved (Mallet et al. 2009). The Sahelian vegetation is highly variable and seasonal

dust sources linked to drying conditions or land cover practice are not accounted for. Dust aerosols have been shown to be important in terms of the precipitation diurnal cycle (Zhao et al. 2011), and they can also have a longer term influence on decadal climate variability via tropical Atlantic SST modifications (Evan et al. 2009). Finally, the present study does not account for microphysical effects of dust, which are proved to be important for ice phase nucleation, possibly impacting convective systems over the Sahel (Crumeyrolle et al. 2008, Tulet et al. 2010) and is also thought to have potential importance in terms of warm microphysics and cloud condensation nuclei (Kumar et al. 2011). We are presently conducting developments aimed at improving emission size distribution as well as dust interactions with gas-phase compounds and other types of aerosols, which is necessary to better represent particle chemical aging and hygroscopic properties.

Acknowledgements. The authors thank R. L. Miller for his valuable comments and advice on the manuscript.

LITERATURE CITED

- Afiesimama EA, Pal JS, Abiodun BJ, Gutowski WJ, Adedoyin A (2006) Simulation of West African monsoon using the RegCM3. I. Model validation and interannual variability. *Theor Appl Climatol* 86:23–37
- Artale V, Calmanti S, Carillo A, Dell'Aquila A and others (2010) An atmosphere–ocean regional climate model for the Mediterranean area: assessment of a present climate simulation. *Clim Dyn* 35:721–740
- Cavazos C, Todd MC, Schepanski K (2009) Numerical model simulation of the Saharan dust event of 6–11 March 2006 using the Regional Climate Model version 3 (RegCM3). *J Geophys Res* 114:D12109. doi:10.1029/2008JD011078
- Crumeyrolle S, Gomes L, Tulet P, Matsuki A, Schwarzenboeck A, Crahan K (2008) Increase of the aerosol hygroscopicity by cloud processing in a mesoscale convective system: a case study from the AMMA campaign. *Atmos Chem Phys* 8:6907–6924
- Dickinson RE, Henderson-Sellers A, Kennedy PJ (1993) Biosphere–Atmosphere Transfer Scheme (BATS) version 1e as coupled to the NCAR Community Climate Model, Tech Rep Nat Center for Atmospheric Research, Boulder, CO
- Emanuel KA, Zivkovic-Rothman M (1999) Development and evaluation of a convection scheme for use in climate models. *J Atmos Sci* 56:1766–1782
- Evan AT, Vimont DJ, Bennartz R, Kossin JP, Heidinger AK (2009) The role of aerosols in the evolution of tropical North Atlantic Ocean temperature. *Science* 324:778–781
- Giorgi F, Pal SC, Bi X, Sloan L, Elguindi N, Solmon F (2006) Introduction to the TAC special issue: the RegCM3 network. *Theor Appl Climatol* 86:1–4
- Giorgi F, Mearns LO (1999) Introduction to special section: regional climate modeling revisited. *J Geophys Res* 104: 6335–6352
- Grell GA (1993) Prognostic evaluation of assumptions used by cumulus parameterizations. *Mon Weather Rev* 121: 764–787
- Hsu NC, Tsay S, King M, Herman JR (2006) Deep blue retrievals of Asian aerosol properties during ACE-Asia. *IEEE Trans Geosci Rem Sens* 44:3180–3195
- Huffman GJ, Adler RF, Bolvin DT, Gu G and others (2007) The TRMM Multi-satellite Precipitation Analysis (TMPA): quasi-global, multi-year, combined-sensor precipitation estimates at fine scale. *J Hydrometeorol* 8:38–55
- Jones C, Mahowald N, Luo C (2003) The role of easterly waves on African desert dust transport. *J Clim* 16: 3617–3628
- Klüser L, Holzer-Popp T (2010) Relationships between mineral dust and cloud properties in the West African Sahel. *Atmos Chem Phys* 10:6901–6915
- Kok JF (2011) A scaling theory for the size distribution of emitted dust aerosols suggests climate models underestimate the size of the global dust cycle. *Proc Natl Acad Sci USA* 108:1016–1021
- Konare A, Zakey AS, Solmon F, Giorgi F, Rauscher S, Ibrah S, Bi X (2008) A regional climate modeling study of the effect of desert dust on the West African monsoon. *J Geophys Res* 113:D12206. doi:10.1029/2007JD009322
- Kumar P, Sokolik IN, Nenes A (2011) Measurements of cloud condensation nuclei activity and droplet activation kinetics of fresh unprocessed regional dust samples and minerals. *Atmos Chem Phys* 11:3527–3541
- Lau KM, Kim MK, Sud YC, Walker GK (2009) A GCM study of the response of the atmospheric water cycle of West Africa and the Atlantic to Saharan dust radiative forcing. *Ann Geophys* 27:4023–4037
- Lavaysse C, Chaboureaud JP, Flamant C (2011) Dust impact on the West African heat low in summertime. *QJR Meteorol Soc* 137:1227–1240
- Legates DR, Willmott CJ (1990) Mean seasonal and spatial variability in global surface air temperature. *Theor Appl Climatol* 41:11–21
- Liao H, Seinfeld JH (1998) Radiative forcing by mineral dust aerosol: sensitivity to key variables. *J Geophys Res* 103:31637–31646
- Malavelle F, Pont V, Mallet M, Solmon F, Johnson B, Leon JF, Lioussé C (2011) Simulation of aerosol radiative effects over West Africa during DABEX and AMMA SOP-0. *J Geophys Res* 116:D08205. doi:10.1029/2010JD014829
- Mallet M, Tulet P, Serça D, Solmon F and others (2009) Impact of dust aerosols on the radiative budget, surface heat fluxes, heating rate profiles and convective activity over West Africa during March 2006. *Atmos Chem Phys* 9:7143–7160
- Martínez Avellaneda N, Serra N, Stammer D, Minnett PJ (2010) Response of the eastern subtropical Atlantic SST to Saharan dust: a modeling and observational study. *J Geophys Res* 115:C08015. doi:10.1029/2009JC005692
- Martonchik JV, Diner DJ, Kahn R, Gaitley B (2004) Comparison of MISR and AERONET aerosol optical depths over desert sites. *Geophys Res Lett* 31:L16102. doi:10.1029/2004GL01987
- Miller RL, Tegen I (1998) Climate response to soil dust aerosols. *J Clim* 11:3247–3267
- Miller RL, Tegen I, Perlwitz J (2004a) Surface radiative forcing by soil dust aerosols and the hydrologic cycle. *J Geophys Res* 109:D04203. doi:10.1029/2003JD004085

- Miller RL, Perlwitz J, Tegen I (2004b) Modeling Arabian dust mobilization during the Asian summer monsoon: the effect of prescribed versus calculated SST. *Geophys Res Lett* 31:L22214. doi:10.1029/2004GL020669
- Osborne SR, Johnson BT, Haywood JM, Baran AJ, Harrison MAJ, McConnell CL (2008) Physical and optical properties of mineral dust aerosol during the Dust and Biomass-burning Experiment. *J Geophys Res* 113:D00C03. doi:10.1029/2007JD009551
- Paeth H, Feichter J (2006) Greenhouse-gas versus aerosol forcing and African climate response. *Clim Dyn* 26:35–54
- Pal JS, Giorgi F, Bi X, Elguindi N and others (2007) Regional climate modeling for the developing world: the ICTP RegCM3 and regCNET. *Bull Am Meteorol Soc* 88:1395–1409
- Perlwitz J, Miller RL (2010) Cloud cover increase with increasing aerosol absorptivity: a counterexample to the conventional semidirect aerosol effect. *J Geophys Res* 115:D08203. doi:10.1029/2009JD012637
- Ratnam JV, Giorgi F, Kaginalkar A, Cozzini S (2009) Simulation of the Indian monsoon using the RegCM3-ROMS regional coupled model. *Clim Dyn* 33:119–139
- Reynolds RW, Rayner NA, Smith TM, Stokes DC, Wang W (2002) An improved *in situ* and satellite SST analysis for climate. *J Clim* 15:1609–1625
- Rodwell MJ, Jung T (2008) Understanding the local and global impacts of model physics changes: an aerosol example. *QJR Meteorol Soc* 134:1479–1497
- Solmon F, Mallet M, Elguindi N, Giorgi F, Zakey A, Konaré A (2008) Dust aerosol impact on regional precipitation over western Africa: mechanisms and sensitivity to absorption properties. *Geophys Res Lett* 35:L24705. doi:10.1029/2008GL035900
- Sow M, Alfaro SC, Rajot JL, Marticorena B (2009) Size resolved dust emission fluxes measured in Niger during 3 dust storms of the AMMA experiment. *Atmos Chem Phys* 9:3881–3891
- Stanelle T, Vogel B, Vogel H, Bäumer D, Kottmeier C (2010) Feedback between dust particles and atmospheric processes over West Africa during dust episodes in March 2006 and June 2007. *Atmos Chem Phys* 10:10771–10788
- Steiner AL, Pal JS, Rauscher SA, Bell JL and others (2009) Land surface coupling in regional climate simulations of the West African monsoon. *Clim Dyn* 33:869–892
- Sud YC, Wilcox E, Lau WKM, Walker GK and others (2009) Sensitivity of boreal-summer circulation and precipitation to atmospheric aerosols in selected regions. 1. Africa and India. *Ann Geophys* 27:3989–4007
- Sylla MB, Coppola E, Mariotti L, Giorgi F, Ruti PM, Dell'Aquila A, Bi X (2010) Multiyear simulation of the African climate using a regional climate model (RegCM3) with the high resolution ERA-interim reanalysis. *Clim Dyn* 35:231–247
- Tegen I, Lacis AA (1996) Modeling of particle influence on the radiative properties of mineral dust aerosol. *J Geophys Res* 101:19237–19244
- Todd MC, Bou Karam D, Cavazos C, Bouet C and others (2008) Quantifying uncertainty in estimates of mineral dust flux: an intercomparison of model performance over the Bodélé Depression, northern Chad. *J Geophys Res* 113:D24107. doi:10.1029/2008JD010476
- Tompkins AM, Cardinali C, Morcrette JJ, Rodwell M (2005) Influence of aerosol climatology on forecasts of the African easterly jet. *Geophys Res Lett* 32:L10801. doi:10.1029/2004GL022189
- Tulet P, Crahan-Kaku K, Leriche M, Aouizerats B, Crumeyrolle S (2010) Mixing of dust aerosols into a mesoscale convective system: generation, filtering and possible feedbacks on ice anvils. *Atmos Res* 96(2–3):302–314
- Tummon F, Solmon F, Liouise C, Tadrass M (2010) Simulation of the direct and semidirect aerosol effects on the southern Africa regional climate during the biomass burning season. *J Geophys Res* 115:D19206. doi:10.1029/2009JD013738
- Wilcox EM, Lau KM, Kim KM (2010) A northward shift of the North Atlantic Ocean Intertropical Convergence Zone in response to summertime Saharan dust outbreaks. *Geophys Res Lett* 37:L04804. doi:10.1029/2009GL041774
- Yoshioka M, Mahowald NM, Conley AJ, Collins WD, Fillmore DW, Zender CS, Coleman DB (2007) Impact of desert dust radiative forcing on Sahel precipitation: relative importance of dust compared to sea surface temperature variations, vegetation changes, and greenhouse gas warming. *J Clim* 20:1445–1467
- Yue X, Liao H, Wang HJ, Li SL, Tang JP (2011) Role of sea surface temperature responses in simulation of the climatic effect of mineral dust aerosol. *Atmos Chem Phys Discuss* 11:1121–1152
- Zakey AS, Solmon F, Giorgi F (2006) Development and testing of a desert dust module in a regional climate model. *Atmos Chem Phys* 6:1749–1792
- Zhao C, Liu X, Ruby Leung L, Hagos S (2011) Radiative impact of mineral dust on monsoon precipitation variability over West Africa. *Atmos Chem Phys* 11:1879–1893
- Zheng XY, Eltahir EAB (1998) The role of vegetation in the dynamics of West African monsoons. *J Clim* 11:2078–2096

Submitted: May 4, 2011; Accepted: August 3, 2011

Proofs received from author(s): February 8, 2012